

Available online at [www.sciencedirect.com](http://www.sciencedirect.com)**ScienceDirect**

Procedia Manufacturing 38 (2019) 991–999

**Procedia**  
MANUFACTURING[www.elsevier.com/locate/procedia](http://www.elsevier.com/locate/procedia)

29th International Conference on Flexible Automation and Intelligent Manufacturing  
(FAIM2019), June 24-28, 2019, Limerick, Ireland.

## Design of a modular solution for an autonomous vehicle for cargo transport and handling

H. D. B. C. L. de Oliveira<sup>a</sup>, R. D. S. G. Campilho<sup>a,b,\*</sup>, F. J. G. Silva<sup>a</sup>

<sup>a</sup>*ISEP-School of Engineering, Rua Dr. António Bernardino de Almeida 431, 4200-072 Porto, Portugal*

<sup>b</sup>*INEGI, Campus da FEUP, Rua Dr. Roberto Frias 400, 4200-465 Porto, Portugal*

---

### Abstract

Due to the globalization of markets, the industrial competitiveness has increased significantly in the recent years. Within this scope, the transportation of products inside industrial parks acquires special relevancy. One of the solutions is the use of autonomous guided vehicles. This work presents the design of a modular autonomous vehicle, capable of carrying heavy loads, which will improve the performance of industrial parks. This is a compact vehicle with low associated costs and good transport speeds. A drive system was designed, which will be capable of transporting the proposed loads. This design was carried out using simulations of the transport with loads, either in plane ground or in an industrial park. A structural analysis to the vehicle was also undertaken by the Finite Element Method, showing the points of the structure that require reinforcement for the different load cases. Finally, the required corrections were implemented, giving to the structure the ability to carry the desired loads. The end result was an autonomous vehicle with capacity to safely transport the imposed loads in the most efficient possible manner.

© 2019 The Authors. Published by Elsevier B.V.

This is an open access article under the CC BY-NC-ND license (<http://creativecommons.org/licenses/by-nc-nd/4.0/>)

Peer-review under responsibility of the scientific committee of the Flexible Automation and Intelligent Manufacturing 2019 (FAIM 2019)

*Keywords:* Autonomous vehicles; Mechanical project; Structural design; Finite Element Method; Drive systems.

---

---

\* Corresponding author. Tel.: +351-939526892; fax: +351-228321159.

*E-mail address:* [raulcampilho@gmail.com](mailto:raulcampilho@gmail.com)

## **1. Introduction**

Due to the globalization of markets, the industrial competitiveness has increased significantly in the recent years. It was necessary to modernize the industrial parks, aiming at the competitiveness of products, by increasing quality, reducing costs and achieving more affordable prices [1]. Within this scope, the transportation of products inside industrial parks acquires special relevancy. When the transportation system is improved, the transported loads will increase and the time between the demand and the availability of the product will be reduced. One of the solutions used to improve the transportation system is the use of automated guided vehicles (AGV). AGV are platforms capable of performing their functions without human intervention, while performing the desired functions, by taking advantage of their analytical, decision and precision capabilities to meet objectives with the least possible failures [2]. These have been used in automated warehouses, industrial parks, distribution centers and ship ports [3]. A recent case of success it is that of Amazon, which greatly improved its productivity in its automated multi-layered warehouses by the introduction of a large number of Kiva robots [4]. These vehicles have the ability to qualitatively and quantitatively improve freight transport. AGV can work uninterruptedly, which promotes an increase of production with a reduction of associated costs, thus reducing the time of return on investment [5]. AGV can also lead to increased operational safety, since many people gets injured or can even die due of human errors in conventional vehicles, such as driver's distractions, reckless driving, poor driving skills and violations of traffic rules [6]. On the other hand, AGV are expected to stand out in the road recognition, decision and driving skills [7]. The main reason why AGV are not yet widespread in roads and industrial applications are mainly founded on the multitude of scenarios and real life conditions that these vehicles will face in operation. There are three types of AGV: scripted, supervised and intelligent [8]. The former uses a pre-planned script with a template to achieve the goal. Supervised AGV automate some or all of the functions of sensing, planning and networking to perform the activities associated with a stand-alone vehicle, while also taking advantage of the human operator to better understand the sensor data. Intelligent AGV use intelligent autonomy technology to receive and interpret the information acquired by the sensors and make the necessary decisions in order to fulfil their objective [8]. Different authors addressed the development of AGV from different perspectives. Peng et al. [9] describes the mechanical design process, including the control system, of a mobile material conveying robot, which included a chassis driven by four wheels and assisted with omni-directional mobility.

This work presents the design of a modular autonomous vehicle capable of carrying heavy loads, which will improve the performance of industrial parks. This is a compact vehicle with low associated costs and good transport speeds. A drive system was designed, which will be capable of transporting the proposed loads. This design was carried out using simulations of the transport with loads, either in plane ground or in an industrial park. A structural analysis to the vehicle was also undertaken by the Finite Element Method, showing the points of the structure that require reinforcement for different load cases. Finally, the required corrections were implemented, giving to the structure the ability to carry the desired loads.

## **2. Problem statement**

This project aims to develop an autonomous guided vehicle, based on a modular platform concept. Regarding the structure, the challenge is to give the platform the capacity to transport eight tons. This challenge is faced through the design of an additional platform to the existing design, where the loads will be transported, and checking if the capacity of the already developed platform is enough to carry the required loads. For the selection of the drive system and the transmission, the following questions are raised: (1) Is it possible, with the existing platform, to carry the loads that an industrial truck carry? and (2) Does it make sense to be presenting a technology with a higher price in a market where products with the same function are already available with a lower cost of acquisition?

The objective of this paper is to present the design concept for the structure and the drive system of the vehicle, so that it can function as an industrial vehicle of load transportation. Moreover, this work adds another valence to the original platform, which reinforces the bet in the modularity to which it is associated, since the platform was designed to be an aggregator of mobility services.

### 3. Vehicle design

#### 3.1. The final proposal

This project starts from an electric and modular platform designed to be an aggregator of mobility services that is being currently developed. This work aims to resize different components of the platform, making it capable to serve also as a vehicle for transporting materials in industrial parks. The platform is divided in different modules, depending on their position and function in the structure: suspension, upper platform, front, central and rear modules.

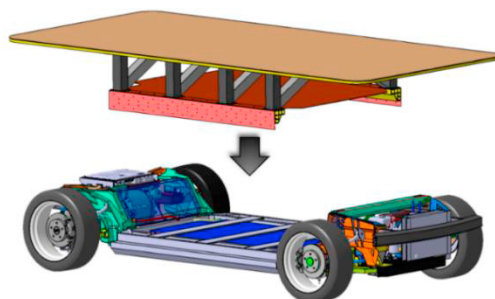


Figure 1 - Final proposal

The assembled set of all components is shown in Figure 1. For steels, forging, milling, and cold or hot rolling were used. Laminating a cold steel, or machining, can present high costs, but the main goal is to keep the parts close to the original design and ensure that they are able to withstand the loads. Therefore, these were the production processes selected because of the fatigue resistance properties they present, in order to avoid deviations from the original design and the design of parts with too large dimensions. In Figure 1 it is possible to verify the lower platform, that is being currently developed, and the superior platform, developed in this work with the intention of being a mean of transmission of the loads transported to the existing platform. When designing the superior platform, the need to transmit the loads to the different modules was taken into account. Therefore, the design process was guided by the following considerations: (1) support the platform in the upper horizontal plate in the front and rear modules, (2) create a sidebar that fits in the central module and (3) distribute the supports between the side bar and the top plate.

#### 3.2. Design process

This Section addresses the AGV design process undertaken. To develop this vehicle, it is proposed that the structure is capable of guaranteeing the transport of 8 tons in the vehicle and 20 tons in tow. For the purpose of designing and optimizing the different equipment groups, numerical analyses were done by the Finite Element Method.

##### 3.2.1. Transmission and drive systems

The electric motor selection is performed by comparing the resisting loads to the movement of the vehicle with the longitudinal force that the motor can produce. To ensure compliance with the imposed requirements, it was necessary to undertake a research on different electric motors. The analysis was divided into five studies (Figure 2), to analyze how the motors behave in the different load cases. In study 1, for instance, the drive system must be capable of carrying the 28 tons, corresponding to the maximum load. It must also be able of climb ramps with slopes up to 5%.

Study 1	Study 2	Study 3	Study 4	Study 5
<ul style="list-style-type: none"> <li>• 28 ton.</li> <li>• 5%</li> </ul>	<ul style="list-style-type: none"> <li>• 11 ton.</li> <li>• 10%</li> </ul>	<ul style="list-style-type: none"> <li>• 4 ton.</li> <li>• 17%</li> </ul>	<ul style="list-style-type: none"> <li>• 2 ton.</li> <li>• 23%</li> </ul>	<ul style="list-style-type: none"> <li>• 0 ton.</li> <li>• 0%</li> </ul>

Figure 2 - Drive system case study

By comparing the velocity values that the different motors can achieve, the transmission ratio and the necessary powers, it is possible to select the ones that appear to be better to fulfil the case studies. When analyzing these criteria, it was possible to verify that two motors had the best performance: Zytek 70 kW and Brusa HSM – 10.17.12.

It was also necessary to carry out an autonomy study, in order to understand how the motors behave with different configurations of drive systems, simulated in situations more similar to reality. Two autonomy studies were done:

- Always travel in plane, with only one battery charge;
- 1,700-meter run, carrying 20 tons, where there are six load cases: climb a ramp, work flat and descend a ramp, all of these either loaded or empty. This study was also divided in the following:
  - Quantity of cargo transported in 8 hours;
  - Quantity of cargo transported per year;
  - Amount of charge carried over the life cycle of the battery.

Figure 3 shows the different configurations simulated in this vehicle. The reference values are estimated from an existing motor solution for a vehicle applied in these situations. The lead-acid battery used is characterized by a capacity of 67.2 kWh, it costs 12720 € and it has a useful life of 600 cycles. The lithium-ion battery used presents a capacity of 30.5 kWh, it costs 28891 € and can be used during 2 500 cycles.

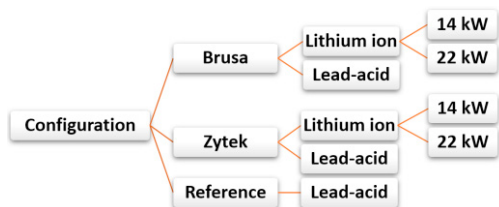


Figure 3 - Different drive system configurations

Figure 4 shows the results of the autonomy study in plane running, in which it is possible to verify the distance travelled with only one battery charge. The corresponding calculations are explained next. Having as variables the elapsed time, the distance, the velocity and the transported loads, it was possible to obtain the resistance force on the wheels. Knowing the resistance force and the time, the required power on the wheels was calculated. With the power on the wheels and the efficiency of the different components between the wheels and the motor, the entry power in the motor was estimated. The entry power in the motor is the same of the supplied power. As such, using supplied power and the time, it was possible to determine the energy to move the vehicle, depending on the distance. Doing an association between the required energy to move the vehicle and the battery capacity, the total distance was found.

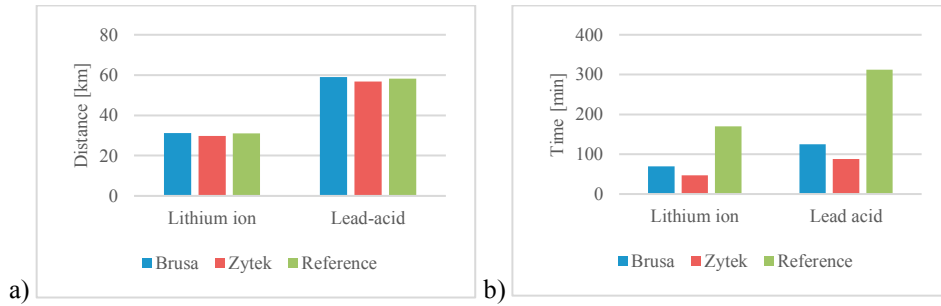


Figure 4 - Results of distance travelled in plane (a) and battery usage time (b)

Figure 4 (a) shows that using the lead-acid battery almost doubles the travelled distances compared to the lithium-ion battery. These results are expected due to the on-board energy difference that the batteries present. When comparing the distances travelled by the different motors, it is possible to verify that, regardless of the power supply, in this study the distances are similar. In addition to the values of distance travelled, the discharge time is also evaluated, by doing an association between the travel time, the required energy to move the vehicle and the battery capacity. The obtained results are shown in Figure 4 (b). Figure 4 (b) shows that the lithium-ion battery lasts just over half the time of the lead-acid battery. But, by crossing these data with that of Figure 4 (a), it can be concluded that the reference vehicle takes 3 times longer to exhaust the energy, for similar distances. This is because the reference motor has a maximum speed of  $\approx 1/3$  that the other motors can develop. Analyzing the performance graphics, it can be concluded that the select drive system is cheaper and more efficient than those currently used.

Using the same method applied to calculate the distance and the battery usage time, but now using the slope as other variable, it can be estimated how much time it takes to discharge the battery and how much distance it will run during one battery charge. Knowing the distance travelled, the battery discharge time and the battery charging time, it is possible to calculate the final distance travelled at the end of a working day, i.e. during 8 h (Figure 5 a).

At this point, the distance travelled per day, the energy needed, the cost of the energy the cost and the useful life of the battery are known. Converting the charges and discharges of the battery in number of cycles, it is possible to know how many days the battery will work. With this, it is possible to know how much loads it will transport during its life cycle and with how much energy. With the cost of the energy, the acquisition cost of the equipment's and the transported loads it is possible to estimate the cost per ton presented in the different motors.

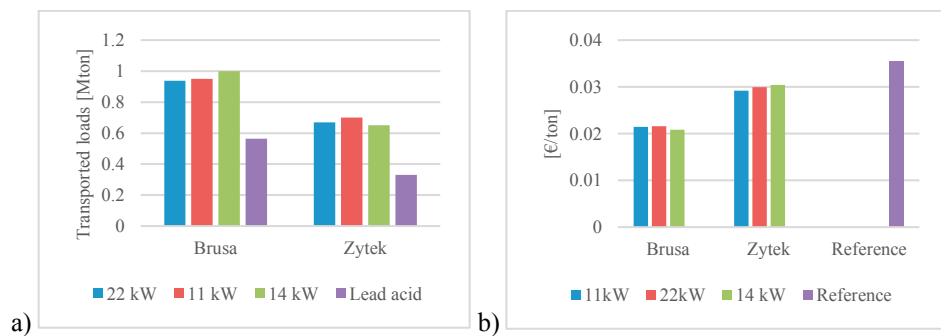


Figure 5 – Transported loads (a) and costs associated with transportation (b)

The Brusa is the motor that stands out, since it presents the lowest energetic cost per transport, and the highest value of load carried with lithium ion battery. These data are reflected in the ability to better amortize the cost of acquiring the battery. The differences in Figure 5 (b) appear to be minimal, but when moving many tons per day, these correspond to a very significant cost reduction. Regarding the cost per year, in the part of the battery acquisition, there is a cost reduction of at least € 806 when the Brusa motor is used. The energy cost per ton is less

0.2 cents, but given that this AGV carries thousands of tons per day, this will be a considerable amount at the end of the year.

### 3.2.2. Load distribution

After select the drive system, it was necessary to check whether the vehicle structure would be able to support the loads that an industrial vehicle needs to transport. The platform design is performed under fatigue, with a life expectancy of at least 300 000 cycles (supercritical fatigue), carrying 8 tons. In order to carry out this selection, different loading cases were simulated: **Design 1** – Static case, loading and unloading cycles; **Design 2** – Curve at maximum speed, with a curvature radius of 20 meters; **Design 3** – Maximum forward acceleration capability and **Design 4** – Braking during forward motion with a deceleration of 3 m/s<sup>2</sup>.

After a fatigue design, through the different load cases presented, two verifications were undertaken: simulation of the speed bump test in each axle, with a vertical acceleration of 3 g (verification 1) and a braking fatigue test, with a deceleration of 2 m/s<sup>2</sup> during rear motion (verification 2). To design the structure, it is necessary to study the forces that develop between the soil and the structure, in order to apply the same forces in the simulation of the various load cases, and to be able to understand how the structure reacts. For the different cases, the load distributions presented in each design were calculated by a static loads and moments analysis. The simulation of the load distributions for the four design scenarios and two verifications resulted in the forces applied to the wheels presented in Table 1 (x – longitudinal axis, y – transverse axis, z – vertical axis).

Table 1 – Calculated load distributions (in N) for the four design scenarios and two verifications.

	Wheel	Left front	Right front	Left back	Right back	
Design 1	Force x	0	0	0	0	
	Force y	0	0	0	0	
	Force z	22 367	22 367	21 777	21 777	
Design 2	Force x	0	0	0	0	
	Force y	-7 490	-12 848	-7 221	-12 579	
	Force z	16 475	28 260	15 884	27 669	
Design 3	Force x	0	0	-7 013	-7 013	
	Force y	0	0	0	0	
	Force z	21 160	21 160	22 985	22 985	
Design 4	Force x	8 847	8 847	5 330	5 330	
	Force y	0	0	0	0	
	Force z	24 810	24 810	19 334	19 334	
Verification 1	Front	Force x	0	0	0	
		Force y	0	0	0	
		Force z	67 103	22 367	21 777	21 777
Verification 2	Rear	Force x	0	0	0	
		Force y	0	0	0	
		Force z	22 637	22 367	65 331	21 777
Verification 2		Force x	3 988	3 988	5 011	5 011
		Force y	0	0	0	0
		Force z	2 817	20 817	23 327	23 327

For design 1, it can be verified that only loads in the Z axis exist, which is expected, since this is a simulation in which there are no velocity variations or curves. It can be confirmed that the center of mass is closer to the front of the vehicle, since the forces applied on the front axle are higher. The obtained data for the design 2 reveals that in the Y and Z axes directions, the forces acting on the left wheels are lower than those applied to the right wheels, due to the transfer of forces caused by the centrifugal force generated by the curve. In the third design it is visible that, applied to the X axis, only forces in the rear axle exist, due to the fact that the vehicle has rear wheel drive. The forces in the X axis are equal between wheels due to using a simple differential, which imposes this condition. In the Z axis, the rear axle is subjected to higher force values. The difference between the forces between axes may seem small, but it is necessary to take into account that, in the first design step, it was verified that the front axle presents higher loads. For design 4, the calculation of the braking forces in the X axis was identical to the mass distribution between the vehicle's axles, in order to simplify the simulation of braking, which was considered as a simple braking system. The loads on the front axle are much higher than the loads on the rear axle. With this distribution of

loads, it is expected that the front suspension and the front module, are the most loaded and those that need more attention.

The resulting forces for verification 1 (front) applied in each simulation were obtained through the simulation of the design 1. In verification 2, there are no differences between the left and right sides due to the symmetry of the structure and the control needed to avoid uncontrolled braking that would cause the vehicle to lose control.

### 3.2.3. Components design

The design of the structure is performed considering fatigue criteria and is simulated in the CATIA V5 software, using the Generative Structural Analysis module. In this simulation the used mesh is addressed as Octree Tetrahedron Mesh, with 3 dimensional elements that present the form of a tetrahedron with 4 nodes. Depending on the geometry, the elements can be parabolic, in which they adapt the best possible to the model, creating one more node in each edge, or linear, in which the elements are pure tetrahedral.

To simplify the simulations by Finite Elements, the modules were divided according to the type of connections between them. The welds are considered perfect connections and whenever there is a non-welded connection, there is a division of the modules. The interactions can be divided into two large groups, virtual connections and connections. Virtual Connections are divided into: ductile virtual connections, rigid virtual connections and ductile virtual springs. Connections are divided into: slider, contact, pressure fitting and virtual bolt tightening. After applying all the interactions, the mesh refinement was performed taking into account the case of static load of eight tons. The simulation has the ability to vary the mesh size depending on the geometry of the part, by using the curvature that is imposed when the mesh parameters are being defined. In addition to the refinement that the software is capable of performing, the mesh has been refined locally whenever it is seemed to be necessary and the software allows it. The study of mesh refinement was performed for the various parts, but only the one of the right rear knuckle, shown in Figure 6, is presented here. The mesh refinement study of the knuckle is revealed in Table 2.

Table 2 - Right rear knuckle mesh refinement study

Element size [mm]	Displacement [mm]	von Mises [Pa]
22	3.22	$2.88 \times 10^8$
20	3.51	$5.50 \times 10^7$
15	3.79	$9.06 \times 10^7$
13	3.78	$4.71 \times 10^7$
11	3.81	$1.29 \times 10^8$
10	3.81	$5.97 \times 10^7$
9	3.80	$7.13 \times 10^7$



Figure 6 – Right rear knuckle mesh

Analyzing Table 2, it is possible to verify that, from the mesh size of 15 mm, the displacements began to converge. Even so, the refinement was taken up to 9 mm in order to obtain the most accurate results possible. When evaluating the von Mises stress variation, it is possible to verify that the stresses do not converge. The non-convergence of the stresses at this point is due to the singularity of this point, where the stresses theoretically tend towards infinity.

### 3.2.4. Design verification

The designs were carried out taking into account the load cases already presented and the forces obtained by the load distribution. All the allowable stresses are estimated taking in count the Gerber failure criterion [10]. Due to space limitations, only one example of design 1 results is presented. The color scale used in the simulations images is made up to the allowable stresses of each part, which can be fatigue or yield depending on the design. The images of the simulations in which the parts are already designed have zones in red. These zones only appear because the installed loads are close to the allowable stress, but never above, except for the holes. The design criteria are presented in section 3.2.2. The first design was carried out taking into account the loading and unloading of eight tons. The suspension arms have been designed to be equal in both the front and rear suspension, thus increasing the number of equal parts produced and reducing the cost of production. The rear suspension support, shown in Figure

7, is an aluminum, which results in low fatigue limit stresses. During this design, the part was yielding at the suspension spring attachment zone and at the lower arm support zone. Figure 7 (a) shows that it was necessary to increase the thickness so as to withstand the applied stresses. Figure 7 (b) shows that, in addition to increasing the thickness of the suspension support, it was also necessary to increase the thickness of the diagonal support.

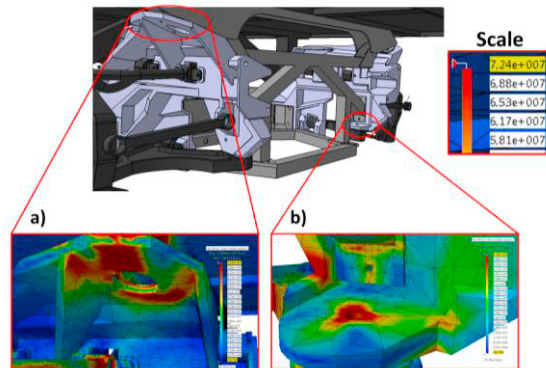


Figure 7 - Rear suspension: a) upper suspension support and b) lower suspension support

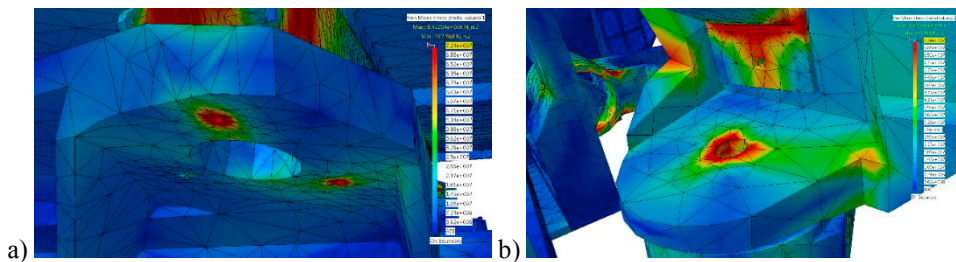


Figure 8 – Design of the rear suspension: a) upper suspension support and b) lower suspension support

Figure 8 shows that, after the thickness was increased, the component was able to support the applied loads. The entire structure was duly designed and verified, to guarantee the transportation capacity of the eight tons. The initial mass of the vehicle was 1318 kg. After the designing done, the final mass is 1394 kg, which results in increased mass of 6%. A more general analysis allows to conclude that, with some changes in the suspension and its supporting components, the structure is able to withstand the imposed load cases.

#### 4. Conclusions

In the study of the drive system, different electric motors on the market were analyzed, and a study of speeds and transmission ratios was made in order to select the motors. After selecting two motors, different configurations were presented with variations of motor, battery and charging power. The different configurations were studied and the configuration of the drive system that seemed more suitable for the developed AGV was selected. The selected configuration shows the Brusa motor - HSM-10.17.12. In the selection of the battery, the most efficient was lithium ion. This battery, when compared to the batteries that are currently used in the market (lead-acid), presents a higher acquisition cost, but it carries much more loads throughout its useful life, which makes it much more profitable. Analyzing the performance graphics, it can be concluded that the select drive system is cheaper and more efficient than those currently used. After testing the structure to the different load cases, it was possible to realize that not all the original structure is able to withstand the required loads. Thus, by modifying the suspension and making some modifications to the parts that support the suspension, the developed platform is capable of transporting the 8 tons.



The increase in mass of the structure was only 6% of the initial mass, which resulted in a total of 1394 kg of final mass of the structure.

## References

- [1] J.M. Rosario. *Automação industrial*. São Paulo, Brasil: Editora Baraúna; 2009.
- [2] A. Al-Mayyahi, W. Wang, P. Birch, Adaptive Neuro-Fuzzy Technique for Autonomous Ground Vehicle Navigation, *Robotics*, 3 (2014) 349.
- [3] T. Le-Anh, M. De Koster, A review of design and control of automated guided vehicle systems, *European Journal of Operational Research*, 171 (2006) 1-23.
- [4] P.R. Wurman, J.M. Romano, The Amazon Picking Challenge 2015 [Competitions], *IEEE Robotics & Automation Magazine*, 22 (2015) 10-2.
- [5] *Automated Guided Vehicles*. Scott Automation; 2018.
- [6] J. Cui, L.S. Liew, G. Sabaliauskaite, F. Zhou, A Review on Safety Failures, Security Attacks, and Available Countermeasures for Autonomous Vehicles, *Ad Hoc Networks*, (2018).
- [7] D.J. Fagnant, K. Kockelman, Preparing a nation for autonomous vehicles: opportunities, barriers and policy recommendations, *Transportation Research Part A: Policy and Practice*, 77 (2015) 167-81.
- [8] N.S. Board, N.R. Council. *Autonomous vehicles in support of naval operations*: National Academies Press; 2005.
- [9] T. Peng, J. Qian, B. Zi, J. Liu, X. Wang, Mechanical Design and Control System of an Omni-directional Mobile Robot for Material Conveying, *Procedia CIRP*, 56 (2016) 412-5.
- [10] J.E. Shigley. *Shigley's mechanical engineering design*. New York, USA: Tata McGraw-Hill Education; 2011.